TECHNISCHE UNIVERSITÄT
KAISERSLAUTERN

SCHRIFTEN ZUR

FUNKTIONALANALYSIS
UND GEOMATHEMATIK

Carsten Mayer

Wavelet Modelling of the Spherical Inverse Source Problem with Application to Geomagnetism

Bericht 5 – Dezember 2003

FACHBEREICH MATHEMATIK

Wavelet Modelling of the Spherical Inverse Source Problem with Application to Geomagnetism

Carsten Mayer

TU Kaiserslautern
Geomathematics Group
67653 Kaiserslautern
P.O. Box 3049
Germany

phone: ++49 631 205-4582
fax: ++49 631 205-4736
email: cmayer@mathematik.uni-kl.de
www: http://www.mathematik.uni-kl.de/∼wwwgeo

Abstract

The article is concerned with the modelling of ionospheric current systems from induced magnetic fields measured by satellites in a multiscale framework. Scaling functions and wavelets are used to realize a multiscale analysis of the function spaces under consideration and to establish a multiscale regularization procedure for the inversion of the considered vectorial operator equation. Based on the knowledge of the singular system a regularization technique in terms of certain product kernels and corresponding convolutions can be formed.
In order to reconstruct ionospheric current systems from satellite magnetic field data, an inversion of the Biot-Savart's law in terms of multiscale regularization is derived. The corresponding operator is formulated and the singular values are calculated. The method is tested on real magnetic field data of the satellite CHAMP and the proposed satellite mission SWARM.

AMS Classification. 42C40, 65R32, 65Z05, 86A20

Key words. Multiscale Regularization, Vectorial Inverse Problems, Biot-Savart Operator

1 Introduction

If looking for first results concerning a mathematical treatment of ionospheric current systems and the corresponding magnetic fields it is inevitable to have a look at the considerations in [14]. In this book both, the ionospheric current systems at the lower ionosphere (110 km) and the induced magnetic field on a sphere above are developed in a Fourier series in terms of spherical harmonics (called Gauss representation, due to [12]). The corresponding Fourier coefficients of both fields can be connected in an analytic way. This way of modelling effects of ionospheric currents and magnetic fields seems to be not the best way nowadays if thinking of the changed geomagnetic data situation and the improved knowledge of the ionosphere. This article gives an improved tool for modelling and reconstructing ionospheric current system from corresponding magnetic field data on different spatial scales.

Reasonably modelling the geomagnetic field on global or regional scales requires dense and homogeneous vectorial data sets. As regards the subject of global and dense coverage, satellites orbiting the Earth in low, near-polar orbits provide firm basis for acquiring the necessary high resolution observations. The German CHAMP satellite mission which started in summer 2000 is, besides other tasks, designed for highly accurate geomagnetic field mapping.

But, it is not only essential to have available adequate data sets, it is also necessary to have at hand the appropriate mathematical tools allowing reasonable analysis of the field data. Kernel functions such as scaling functions and wavelets reflect the small scale spatial variability of ionospheric currents and the induced magnetic field. For a comprehensive introduction of kernel functions the reader is referred to [7], [8], [10] or [16]. Since both the magnetic field and the current system are vector fields the natural way of modelling these fields is by tensor kernel function and linear tensor convolutions (see [8], [18]). This linear technique is circumvented in this article by an equivalent bilinear two step method using vector kernel functions two different convolutions. Similar approaches have already been proposed in [2], [9] or [16]

The outline of this article is as follows. First of all we give the necessary notation. Additionally, two complete and closed orthonormal systems in the space of square integrable spherical vector fields are presented. These systems of vector spherical harmonics give the foundation for the multiscale modelling of vector fields in the following sections.
Section 3 gives a general approach to the theory of multiscale regularization techniques of vectorial inverse problems. We present, how regularization vector scaling functions and wavelets are constructed and develop the aforementioned bilinear two step method for regularization.
In Section 4 the 'inverse source problem' is introduced, i.e. the reconstruction of ionospheric current systems corresponding to given magnetic field data. An ansatz of how this problem can be modelled involving satellite geometries is presented. The necessary tools (such as the singular system of the corresponding operator) are derived in order to use the multiscale technique presented in Section 3.
Section 5 deals with the application of our multiscale method of reconstructing current system from magnetic field data to data sets of two different satellite missions, i.e. to

CHAMP satellite data and to simulated magnetic field data of the proposed SWARM mission.

2 Preliminaries

In this section the reader is provided with the essential tools used in the course of this article. We start with introducing some basic notation and the nomenclature which is used in our considerations.

2.1 Notation

During the course of this article we will permanently be confronted with scalar which are denoted by capital letters (F, G, etc) and vector fields which are symbolized by lower-case letters (f, g, etc).

A sphere of radius R centered around the origin is denoted by $\Omega_R = \{x \in \mathbb{R}^3 \,|\, |x| = R\}$. In particular, $\Omega = \Omega_1$ is the *unit sphere* in $\mathbb{R}^3$. We set Ω_R^{int} for the 'inner space' of Ω_R, $\Omega_R^{int} = \{x \in \mathbb{R}^3 \,|\, |x| < R\}$ while $\Omega_R^{ext} = \mathbb{R}^3 \setminus \overline{\Omega_R^{int}}$ is the 'outer space' of Ω_R. Clearly, $\Omega_R^{ext} = \{x \in \mathbb{R}^3 \,|\, |x| > R\}$. By $\Omega_{(R_1,R_1)}$ we denote the open spherical shell with inner radius R_1 and outer radius R_2 given by $\Omega_{(R_1,R_2)} = \{x \in \mathbb{R}^3 \,|\, R_1 < |x| < R_2\}$.

In what follows we need a number of differential operators which we introduce next. $\nabla_x = (\partial/\partial x_1, \partial/\partial x_2, \partial/\partial x_3)^T$ denotes the *gradient* in cartesian coordinates in $\mathbb{R}^3$ and ∇^* represents its tangential part, called *surface gradient*. The *Laplace operator* is symbolized by $\Delta = \nabla \cdot \nabla$ and the corresponding tangential operator, called *Beltrami operator*, is given by $\Delta^* = \nabla^* \cdot \nabla^*$. The *curl gradient* L_x is given by $L_x = x \wedge \nabla_x$ with tangential counterpart given by L^* which is called *surface curl gradient*. For more information concerning these operators the reader is referred to [8].
Let f be a tangential vector field with respect to the sphere Ω_R, i.e. $f \cdot \xi = 0$ for all $\xi \in \Omega$. Furthermore, let f possess the component functions F_i, i.e. $f(x) = \sum_{i=1}^3 F_i(x)\epsilon^i$, $x \in \Omega$. Then the *surface divergence* $\nabla^* \cdot$ and the *surface curl divergence* $L^* \cdot$ are defined by

$$\nabla^* \cdot f = \sum_{i=1}^{3} (\nabla^* F_i) \cdot \epsilon^i \,, \quad L^* \cdot f = \sum_{i=1}^{3} (L^* F_i) \cdot \epsilon^i \,.$$

A variety of function spaces will be needed in this article. Let $\mathcal{C}(U)$ be the set of all continuous, real functions defined on the set $U \subset \mathbb{R}^3$, equipped with the standard supremum norm. A function is said to be of class $\mathcal{C}^{(k)}(U), 0 \leq k \leq \infty$, if it is $k-$times continuously differentiable on U. If $U \subset \mathbb{R}^3$ is a measurable subset of $\mathbb{R}^3$, the set of scalar functions $F : U \to \mathbb{R}$ which are measurable and for which

$$||F||_{\mathcal{L}^p(U)} = \left(\int_U |F(x)|^p \, dx \right)^{\frac{1}{p}} < \infty$$

is denoted by $\mathcal{L}^p(U)$, where dx denotes the volume element in U. Note that in the case of $U = \Omega_R$ with radius $R > 0$ we write $d\omega_R(x)$ instead of dx and $d\omega(x)$ instead of $d\omega_1(x)$.

In analogy to the scalar case we define function spaces of vector valued functions. These spaces will normally be symbolized by lower-case letters. Let $c(U)$ be the set of all vector valued, continuous functions $f : U \to \mathbb{R}^n$ defined on the set $U \subset \mathbb{R}^3$, equipped with the norm

$$||f||_{c(U)} = \sup_{x \in U} |f(x)|.$$

A vector field f is said to be of class $c^{(k)}(U), 0 \leq k \leq \infty$, if every component function $f \cdot \epsilon^i$, $i = 1, \ldots, n$, of f is $k-$times continuously differentiable on U. The set of vector fields $f : U \to \mathbb{R}$ which are measurable and for which

$$||f||_{l^p(U)} = \left(\int_U |f(x)|^p \, dx \right)^{\frac{1}{p}} < \infty$$

is denoted by $l^p(U)$.

2.2 Two Sets of Vector Spherical Harmonics

In what follows scalar spherical harmonics are introduced. The approach presented here is based on [8]. Scalar spherical harmonics are restrictions of homogeneous harmonic polynomials in $\mathbb{R}^3$ to the unit sphere. More explicitly, let $H_n : \mathbb{R}^3 \to \mathbb{R}$ be a homogeneous harmonic polynomial of degree n, i.e.

1. H_n is polynomial of degree n in $\mathbb{R}^3$,
2. $H_n(\lambda x) = \lambda^n H_n(x)$ for all $\lambda \in \mathbb{R}$ and $x \in \mathbb{R}^3$ (homogeneity),
3. $\Delta_x H_n(x) = 0$ for all $x \in \mathbb{R}^3$ (harmonicity),

then the restriction $Y_n = H_n|_\Omega$ is called a *scalar spherical harmonic of degree n*. An essential result of the theory of scalar spherical harmonics is the fact that any spherical harmonic $Y_n \, , n \in \mathbb{N}_0 \, ,$ is an infinitely often differentiable eigenfunction of the Beltrami operator Δ^* corresponding to the eigenvalue $-n(n+1) \, , n \in \mathbb{N}_0 \, ,$ i.e.

$$\Delta^*_\xi Y_n(\xi) = -n(n+1) Y_n(\xi), \quad \xi \in \Omega, \quad Y_n \in Harm_n(\Omega), \quad n \in \mathbb{N}_0$$

and vice versa. Throughout the remainder of this work, we denote by $\{Y_{n,k}\}_{k=1,\ldots,2n+1}$ a complete orthonormal system in the space $Harm_n(\Omega)$ with respect to the inner product $(\cdot, \cdot)_{\mathcal{L}^2(\Omega)}$.

The system of spherical harmonics is closed and complete in $\mathcal{L}^2(\Omega)$. For a general definition of closure and completeness and relations between the two terms in Hilbert spaces the reader is referred e.g. to [4]. It is obvious that the system $\{Y^R_{n,k}\} = \{\frac{1}{R} Y_{n,k}(\frac{\cdot}{R})\}$ forms an closed and complete orthonormal system in $\mathcal{L}^2(\Omega_R)$.

In order to construct a system of vector spherical harmonics in the space $l^2(\Omega)$ out of the system of scalar spherical harmonics we introduce the following operators.

Definition 2.1
For $\xi \in \Omega$ and $F \in \mathcal{C}^{(0_i)}(\Omega)$ the operators $o^{(i)} : \mathcal{C}^{(0_i)}(\Omega) \to c(\Omega), i \in \{1, 2, 3\}$, are defined via

$$o^{(1)}_\xi F(\xi) = \xi F(\xi), \quad o^{(2)}_\xi F(\xi) = \nabla^*_\xi F(\xi), \quad o^{(3)}_\xi F(\xi) = L^*_\xi F(\xi).$$

where we have used the abbreviation

$$0_i = \begin{cases} 0 & \text{if } i = 1 \\ 1 & \text{if } i = 2, 3\,. \end{cases}$$

It is clear that $o^{(1)}F$ is a radial vector field, while $o^{(2)}F$ and $o^{(3)}F$ are purely tangential. Furthermore, the operators $o^{(i)}$ can be extended in a canonical way to the space $l^2(\Omega)$.

Motivated by the operators $o^{(i)}$ we will now introduce vector spherical harmonics.
If $\{Y_{n,k}\}_{n=0,1,\ldots;k=1,\ldots,2n+1}$ is an $\mathcal{L}^2(\Omega)-$orthonormal set of scalar spherical harmonics it easily follows by the properties of the $o^{(i)}-$operators (see [8]) that

$$y^{(i)}_{n,k} = (\mu^{(i)}_n)^{-1/2} o^{(i)} Y_{n,k},$$

$i \in \{1,2,3\}, n \geq 0_i; k = 1, \ldots, 2n+1$, forms an $l^2(\Omega)-$orthonormal system of vector spherical harmonics, where the normalization values $\mu^{(i)}_n$ are given by

$$\mu^{(i)}_n = \begin{cases} 1 & \text{if } i = 1 \\ n(n+1) & \text{if } i = 2, 3\,. \end{cases} \tag{1}$$

It is known that the system $\{y^{(i)}_{n,k}\}$ is a complete and closed orthonormal system in $l^2(\Omega)$.According to our construction we get

$$\xi \wedge y^{(1)}_{n,k}(\xi) = 0, \quad \xi \cdot y^{(2)}_{n,k}(\xi) = 0, \quad \xi \cdot y^{(3)}_{n,k}(\xi) = 0,$$
$$L^*_\xi \cdot y^{(2)}_{n,k}(\xi) = 0, \quad \nabla^*_\xi \cdot y^{(3)}_{n,k}(\xi) = 0.$$

To construct a second set of vector spherical harmonics we use the restriction of homogeneous harmonic vector polynomials to the sphere. This system is known from theoretical physics and developed, for example, in [1] or [5]. The introduction of the system given in this article follows mainly the course of [19]. According to our nomenclature a system of vector spherical harmonics is adequately described by the following lemma.

Lemma 2.2
Let $\{Y_{n,k}\}_{\substack{n=0,1,\ldots;\\ k=1,\ldots,2n+1}}$ be an $\mathcal{L}^2(\Omega)-$ orthonormal system of scalar spherical harmonics. Then the vector fields

$$\begin{aligned} u^{(1)}_{n,k} &= (\nu^{(1)}_n)^{-1/2} \left((n+1) o^{(1)} Y_{n,k} - o^{(2)} Y_{n,k} \right), \\ &= \sqrt{\frac{n+1}{2n+1}}\, y^{(1)}_{n,k} - \sqrt{\frac{n}{2n+1}}\, y^{(2)}_{n,k}, \quad n = 0, 1, \ldots; k = 1, \ldots, 2n+1, \end{aligned}$$

$$\begin{aligned} u^{(2)}_{n,k} &= (\nu^{(2)}_n)^{-1/2} \left(n o^{(1)} Y_{n,k} + o^{(2)} Y_{n,k} \right), \\ &= \sqrt{\frac{n}{2n+1}}\, y^{(1)}_{n,k} + \sqrt{\frac{n+1}{2n+1}}\, y^{(2)}_{n,k}, \quad n = 1, 2, \ldots; k = 1, \ldots, 2n+1, \end{aligned}$$

$$u^{(3)}_{n,k} = (\nu^{(3)}_n)^{-1/2} o^{(3)} Y_{n,k} = y^{(3)}_{n,k}, \quad n = 1, 2, \ldots; k = 1, \ldots, 2n+1,$$

form an $l^2(\Omega)-$orthonormal set of vector spherical harmonics with the normalization coefficients given by

$$\nu_n^{(i)} = \begin{cases} (n+1)(2n+1) & \text{for } i = 1, n \in \mathbb{N}_0, \\ n(2n+1) & \text{for } i = 2, n \in \mathbb{N}, \\ n(n+1) & \text{for } i = 3, n \in \mathbb{N}\,. \end{cases}$$

The proof of this lemma easily follows from computations involving the orthonormality of the system $\{y_{n,k}^{(i)}\}$. The reader should note, that the system $\{u_{n,k}^{(i)}\}$ does not separate between radial and tangential fields. However, as we will see later, this system has other advantageous properties in electro- and magnetostatic modelling. A direct consequence of the closure and completeness of the system $\{y_{n,k}^{(i)}\}$ is the following result.

Corollary 2.3
Let the system of vector spherical harmonics $\{u_{n,k}^{(i)}\}_{\substack{i=1,2,3 \\ n=0_i,\ldots;k=1,\ldots,2n+1}}$ be defined as in Lemma 2.2. Then the following statements are valid:

1. *The system of vector spherical harmonics is closed in $c(\Omega)$ with respect to $||\cdot||_{c(\Omega)}$ and $||\cdot||_{l^2(\Omega)}$.*
2. *The system is complete in $l^2(\Omega)$ with respect to $(\cdot,\cdot)_{l^2(\Omega)}$.*

Note that the system of vector spherical harmonics given by

$$u_{n,k}^{(i),R} = \frac{1}{R}\, u_{n,k}^{(i)}, \quad i \in \{1,2,3\};\ n = 0_i, \ldots;\ k = 1, \ldots, 2n+1, \tag{2}$$

establishes a closed and complete orthonormal system in the Hilbert space $l^2(\Omega_R)$.
In the sense of subspaces of the Hilbert space $l^2(\Omega_R)$ the above results may be written as follows.

$$l^2(\Omega_R) = l_{\mathcal{U}}^{2,(1)}(\Omega_R) \oplus l_{\mathcal{U}}^{2,(2)}(\Omega_R) \oplus l_{\mathcal{U}}^{2,(3)}(\Omega_R), \tag{3}$$

with

$$l_{\mathcal{U}}^{2,(i)}(\Omega_R) = \overline{\bigoplus_{n=0_i}^{\infty} span\{u_{n,k}^{(i),R} | k = 1, \ldots, 2n+1\}}^{||\cdot||_{l^2(\Omega_R)}}. \tag{4}$$

For both orthonormal systems $\{y_{n,k}^{(i)}\}$ and $\{u_{n,k}^{(i)}\}$ certain vectorial addition theorems can be formulated (see [8]). The interested reader is referred to [19], where systems of vector spherical harmonics are introduced in a very complete manner.

3 Multiscale Regularization of Vectorial Inverse Problems

In the following section we will give the functional-analytic background and the construction of our multiscale technique for the regularization of vectorial ill-posed problems.

Let $(\mathfrak{h}, (\cdot,\cdot)_{\mathfrak{h}})$ and $(\mathfrak{k}, (\cdot,\cdot)_{\mathfrak{k}})$ be two separable Hilbert spaces of both vector valued functions (with values in $\mathbb{R}^3$) defined on the domain $D_{\mathfrak{h}} \subset \mathbb{R}^m$, respectively, $D_{\mathfrak{k}} \subset \mathbb{R}^m$ and let $g \in \mathfrak{k}$ be given. Then we search the function $f \in \mathfrak{h}$, which is related to g via

$$\Lambda : \mathfrak{h} \to \mathfrak{k}, \quad \Lambda f = g, \tag{5}$$

where the operator Λ is assumed to be bounded, linear and compact with singular system $\{\sigma_n, h_n, k_n\}_{n=0,1,\ldots}$. The sequence $\{\sigma_n^2\}$ form the non-zero eigenvalues of the selfadjoint operator $\Lambda^*\Lambda$ which are assumed to be numbered in descending order. $\{h_n\}$ is a complete orthonormal system in $\overline{\mathcal{R}(\Lambda^*)}^{||\cdot||_{\mathfrak{h}}}$ such that $\Lambda h_n = \sigma_n k_n$, while $\{k_n\}$ denotes a complete orthonormal system in $\overline{\mathcal{R}(\Lambda)}^{||\cdot||_{\mathfrak{k}}}$ such that $\Lambda^* k_n = \sigma_n h_n$.
As is well-known, the problem of solving this operator equation is called *well-posed* in the sense of Hadamard, if for each $g \in \mathfrak{k}$ there exists one and only one $f \in \mathfrak{h}$ with $\Lambda f = g$ (existence and uniqueness of the inverse) and the solution $f \in \mathfrak{h}$ depends continuously on the right hand side $g \in \mathfrak{k}$ (continuity of the inverse). If at least one of these properties is violated, then the problem is said to be *ill-posed* (see e.g. [6] or [15]).

The Picard condition tells us that the problem (5) has a solution if and only if $g \in \mathfrak{k}$ satisfies

$$\sum_{n=}^{\infty} \left(\sigma_n^{-1}(g, k_n)_{\mathfrak{k}}\right)^2 < \infty\,.$$

In practical applications we are generally not concerned with the ideal situation of a well-posed problem. First of all a solution of $\Lambda f = g$ exists only if g is in $\mathcal{R}(\Lambda)$, the range of Λ. Errors due to unprecise measurements result in noisy data which may cause that $g \notin \mathcal{R}(\Lambda)$. The perturbed right hand side will be denoted by g^δ with a known error level given by

$$||g^\delta - g||_{\mathfrak{k}} \leq \delta\,. \tag{6}$$

In order to define a solution even in this case we consider an approximate solution, which occupies the least-squares property, i.e. one seeks that element of $\mathfrak{h}$ solving $\min_{f\in\mathfrak{h}} ||\Lambda f - g^\delta||_{\mathfrak{k}}$. If Λ is injective, the solution of $\min_{f\in\mathfrak{h}} ||\Lambda f - g^\delta||_{\mathfrak{k}}$ is uniquely determined as the orthogonal projection of g^δ onto $\overline{\mathcal{R}(\Lambda)}^{||\cdot||_{\mathfrak{k}}}$, otherwise there exist infinitely many solutions if $g^\delta \in \mathcal{R}(\Lambda)^\perp$. Then we are interested in the least-squares solution which is of minimal norm $||f||_{\mathfrak{h}}$. Determining the desired least-squares solution with minimal norm is equivalent to the determination of the (unique) generalized solution f^+. The generalized inverse for the above problem can be given in terms of the singular system by

$$f^+ = \Lambda^+ g = \sum_{n=0}^{\infty} \sigma_n^{-1}(g, k_n)_{\mathfrak{k}} h_n, \quad g \in \mathcal{R}(\Lambda) \oplus \mathcal{R}(\Lambda)^\perp. \tag{7}$$

However, the described concept of least-squares solution with minimal norm fails, if $g \notin \mathcal{R}(\Lambda) \oplus \mathcal{R}(\Lambda)^\perp$ or the generalized inverse operator Λ^+ is not continuous. Then,

the lack of continuity needs to be replaced by a regularization of Λ^+. In other words, in the situation that only a disturbed right hand side is known instead of g, we are interested in an approximation of the generalized solution f^+ which depends continuously on the given data.

At first we have to define more precisely what is understood by the above mentioned term of regularization.

Definition 3.1
Let $(\mathfrak{h}, (\cdot,\cdot)_{\mathfrak{h}})$ and $(\mathfrak{k}, (\cdot,\cdot)_{\mathfrak{k}})$ be two separable Hilbert spaces and let $\Lambda : \mathfrak{h} \to \mathfrak{k}$ be linear and bounded. Then the family of operators $\Lambda_J : \mathfrak{k} \to \mathfrak{h}$, $J \in \mathbb{Z}$, is called a *regularization* of the generalized inverse Λ^+ if the following conditions are fulfilled:

1. Λ_J is linear and bounded on $\mathfrak{k}$ for all $J \in \mathbb{Z}$.
2. For any $g \in \mathcal{R}(\Lambda) \oplus \mathcal{R}(\Lambda)^{\perp}$, the limit relation

$$\lim_{J\to\infty} ||\Lambda_J g - \Lambda^+ g||_{\mathfrak{h}} = 0$$

holds.

The function $f_J = \Lambda_J g$ is called *J-level regularization* of the problem $\Lambda f = g$ and the parameter J is called *regularization parameter*.

In what follows, the development of the multiresolution analysis for regularization will be based on so-called vector product kernels which are defined next. For the definition we need another separable Hilbert space of scalar valued functions defined over the domain $D_{\mathcal{H}}$ which will be given by $(\mathcal{H}, (\cdot,\cdot)_{\mathcal{H}})$ and which will be called 'park Hilbert space'.

Definition 3.2
Let $(\mathfrak{h}, (\cdot,\cdot)_{\mathfrak{h}})$ and $(\mathcal{H}, (\cdot,\cdot)_{\mathcal{H}})$ be real separable Hilbert spaces of vector, respectively, scalar valued functions over the domain $D_{\mathfrak{h}} \subset \mathbb{R}^m$, respectively, $D_{\mathcal{H}} \subset \mathbb{R}^m$. Let, furthermore, $\{h_n\}_{n\in\mathbb{N}}$ and $\{H_n\}_{n\in\mathbb{N}}$ be corresponding countable, orthonormal and complete systems in $\mathfrak{h}$ and $\mathcal{H}$, respectively. Then, a function $\gamma(\cdot,\cdot) : D_{\mathfrak{h}} \times D_{\mathcal{H}} \to \mathbb{R}^3$ of the form

$$\gamma(x,y) = \sum_{n=0}^{\infty} \gamma^{\wedge}(n) h_n(x) H_n(y), \quad x \in D_{\mathfrak{h}}, y \in D_{\mathcal{H}},$$

is called $(\mathfrak{h},\mathcal{H})-$*vector product kernel* . The sequence $\{\gamma^{\wedge}(n)\}_{n=0,1,\ldots}$ is the *symbol of the vector product kernel*. The symbol is called $(\mathfrak{h},\mathcal{H})-$*admissible* if

$$\sum_{n=0}^{\infty} \left(\gamma^{\wedge}(n) h_n(x)\right)^2 < \infty \quad x \in D_{\mathfrak{h}}, \quad \sum_{n=0}^{\infty} \left(\gamma^{\wedge}(n) H_n(y)\right)^2 < \infty \quad y \in D_{\mathcal{H}}.$$

By the admissibility of the symbol we can conclude that $\epsilon^i \cdot \gamma(x,\cdot) \in \mathcal{H}$ for every fixed $x \in D_{\mathfrak{h}}$ and $i = 1,2,3$, and $\gamma(\cdot,y) \in \mathfrak{h}$ for every fixed $y \in D_{\mathcal{H}}$.

Next, we have to introduce two convolutions, i.e. a decomposition convolution which results in a scalar function and a reconstruction convolution which maps the scalar field back to a vector valued function.

Definition 3.3
Let $\gamma : D_{\mathfrak{h}} \times D_{\mathcal{H}} \to \mathbb{R}^3$ be a vector product kernel with $(\mathfrak{h}, \mathcal{H})-$admissible symbol. The $\mathfrak{h}-$convolution of γ against a vector valued function $f \in \mathfrak{h}$ is defined by

$$(\gamma *_{\mathfrak{h}} f)(y) \;\; = \;\; (\gamma(\cdot, y), f)_{\mathfrak{h}}\,, \quad y \in D_{\mathcal{H}},$$

while the $\star-$convolution of a product kernel γ against a scalar valued function $G \in \mathcal{H}$ is defined by

$$(\gamma \star G)(x) = \sum_{i=1}^{3} \left(\epsilon^i \cdot \gamma(x, \cdot), G\right)_{\mathcal{H}}, \quad x \in D_{\mathfrak{h}}.$$

By the admissibility of the product kernel γ it is clear that

$$(\gamma *_{\mathfrak{h}} f) \in \mathcal{H}, \quad f \in \mathfrak{h}; \qquad (\gamma \star G) \in \mathfrak{h}, \quad G \in \mathcal{H}.$$

Using the orthonormality of the system $\{h_n\}$ in the Hilbert space $\mathfrak{h}$ we easily get

$$\gamma *_{\mathfrak{h}} f = \sum_{n=0}^{\infty} \gamma^{\wedge}(n) f^{\wedge}(n) H_n \tag{8}$$

for $f \in \mathfrak{h}$ in the sense of the $\mathcal{H}-$norm, where $\{f^{\wedge}(n)\}$ are the Fourier coefficients of f with respect to the system $\{h_n\} \subset \mathfrak{h}$. With the same argument we find for $G \in \mathcal{H}$

$$\gamma \star G = \sum_{n=0}^{\infty} \gamma^{\wedge}(n) G^{\wedge}(n) h_n \tag{9}$$

in the sense of the $\mathfrak{h}-$norm where $\{G^{\wedge}(n)\}$ are the Fourier coefficients of G with respect to the system $\{H_n\} \subset \mathcal{H}$.

Based on the definition of a vector kernel and the two convolutions we are now able to construct a regularization as a vector multiresolution analysis of the problem (5). We define regularization vector scaling functions via their symbol as follows.

Definition 3.4
Let the Hilbert spaces $\mathfrak{h}$, $\mathfrak{k}$ and $\mathcal{H}$ be given as above. Furthermore, let $\{(\varphi_J)^{\wedge}(n)\}_{n=0,1,\ldots}$, $J \in \mathbb{Z}$, be $(\mathfrak{h}, \mathcal{H})-$ and $(\mathfrak{k}, \mathcal{H})-$admissible satisfying the following properties:

1. $\lim\limits_{J \to \infty} \left((\varphi_J)^{\wedge}(n)\right)^2 = \sigma_n^{-1}, \quad n \in \mathbb{N},$
2. $\left((\varphi_J)^{\wedge}(n)\right)^2 \geq \left((\varphi_{J-1})^{\wedge}(n)\right)^2, \quad J \in \mathbb{Z},\, n \in \mathbb{N},$
3. $\lim\limits_{J \to -\infty} \left((\varphi_J)^{\wedge}(n)\right)^2 = 0, \quad n \in \mathbb{N}\,.$

Then $\{(\varphi_J)^{\wedge}(n)\}_{n=0,1,\ldots}$ is called the *generating symbol of a regularization vector scaling function*. The family of kernels $\{{}^d\varphi_J\}$, $J \in \mathbb{Z}$, given by

$${}^d\varphi_J(x, y) = \sum_{n=0}^{\infty} (\varphi_J)^{\wedge}(n) k_n(x) H_n(y), \quad x \in D_{\mathfrak{k}}, y \in D_{\mathcal{H}},$$

is called *decomposition regularization vector scaling function* and the family of kernels $\{{}^r\varphi_J\}$, $J \in \mathbb{Z}$, given by

$$ {}^r\varphi_J(x,y) = \sum_{n=0}^{\infty} (\varphi_J)^\wedge(n) h_n(x) H_n(y), \quad x \in D_{\mathfrak{k}}, y \in D_{\mathcal{H}}, $$

is called *reconstruction regularization vector scaling function.*

Different examples of admissible symbols generating regularization scaling functions can be found in [8] or [17]. The symbol which is continuously used throughout this article is the cubic polynomial (CP) regularization symbol given by

$$ (\varphi_J)^\wedge(n) = \begin{cases} \sqrt{\sigma_n^{-1}} \left(1 - n/N_J\right)^2 \left(1 + 2n/N_j\right) & n = 0, \dots N_J, \\ 0 & \text{else}, \end{cases} $$

where $\{N_J\}_{J\in\mathbb{Z}} \subset \mathbb{N}_0$ is a monotonically increasing sequence which might, for example, by chosen dyadic (i.e. $N_J = 2^J$).

Following the definition of regularization vector scaling functions we are led to the following result.

Theorem 3.5
Let $\{(\varphi_J)^\wedge(n)\}_{n=0,1,\dots}$, $J \in \mathbb{Z}$, be the generating symbol of the regularization vector scaling functions ${}^d\varphi_J$ and ${}^r\varphi_J$, respectively, as given in Definition 3.4. Then the sequence of operators Λ_J, $J \in \mathbb{Z}$, defines a regularization in the sense of Definition 3.1, i.e.

$$ \lim_{J\to\infty} ||f_J - \Lambda^+ g||_{\mathfrak{h}} = 0 $$

holds for all $g \in \mathcal{R}(\Lambda) \oplus \mathcal{R}(\Lambda)^\perp$ with $\Lambda f = g$, where $\Lambda_J g = f_J$, given by

$$ f_J = \Lambda_J g = {}^r\varphi_J \star ({}^d\varphi_J *_{\mathfrak{k}} g), \tag{10} $$

is said to be the J-level approximation of $\Lambda^+ g$.

For a proof of this theorem in the scalar case the reader is referred to [10] and in the vector case to [17].

From now on the whole theory of multiresolution by spherical wavelets (see [8]) can be transferred to the case of regularization of vectorial inverse problems by vector scaling functions and wavelets. We can define decomposition and reconstruction regularization vector wavelets and give a wavelet regularization theorem. We will just give some important facts of regularizing vector wavelet theory and regularizing vector multiresolution analysis at this point.

Definition 3.6
Let $\left\{(\varphi_J)^\wedge(n)\right\}_{n=0,1,\dots}$, $J \in \mathbb{Z}$, be the generating symbol of a regularization scaling function. Then the generating symbol $\left\{(\psi_J)^\wedge(n)\right\}_{n=0,1,\dots}$, $J \in \mathbb{Z}$, of the associated regularization wavelet is defined via the refinement equation

$$ (\psi_J)^\wedge(n) = \left((\varphi_{J+1})^\wedge(n)^2 - (\varphi_J)^\wedge(n)^2\right)^{1/2}, \quad n \in \mathbb{N}_0. \tag{11} $$

The family $\left\{{}^{d}\psi_J\right\}$, $J \in \mathbb{Z}$, of kernels given by

$$ {}^{d}\psi_J(x,y) = \sum_{n=0}^{\infty} (\psi_J)^{\wedge}(n) k_n(x) H_n(y), \quad x \in D_{\mathfrak{k}},\ y \in D_{\mathcal{H}}, $$

is called *decomposition regularization vector wavelet*, whereas the family $\{{}^{r}\psi_J\}$, $J \in \mathbb{Z}$, of kernels given by

$$ {}^{r}\psi_J(x,y) = \sum_{n=0}^{\infty} (\psi_J)^{\wedge}(n) h_n(x) H_n(y), \quad x \in D_{\mathfrak{h}}, y \in D_{\mathcal{H}}, $$

is called *reconstruction regularization vector wavelet*.

Next, we will give the analogue to Theorem 3.5 for regularization of the problem (5) in terms of wavelets.

Theorem 3.7
Let $\{(\varphi_J)^{\wedge}(n)\}_{n=0,1,\ldots}$, $J \in \mathbb{Z}$, be the generating symbol of a regularization vector scaling function. Suppose that $\{(\psi_J)^{\wedge}(n)\}_{n=0,1,\ldots}$, $J \in \mathbb{Z}$, is the generating symbol of the associated regularization vector wavelet. Furthermore, let g be of class $\mathcal{R}(\Lambda) \oplus \mathcal{R}(\Lambda)^{\perp}$ with $\Lambda f = g$. Then

$$ f_J = {}^{r}\varphi_0 \star ({}^{d}\varphi_0 *_{\mathfrak{k}} g) + \sum_{j=0}^{J-1} {}^{r}\psi_j \star ({}^{d}\psi_j *_{\mathfrak{k}} g) $$

is the J-level approximation of $\Lambda^{+}g$ satisfying

$$ \lim_{J\to\infty} ||f_J - \Lambda^{+} g||_{\mathfrak{h}} = 0. $$

The proof of this theorem immediately follows from Definition 3.6 of a regularization wavelet and Theorem 3.5. At last, we give the important fact of a vectorial multiresolution for the regularization case.

Theorem 3.8
The scale spaces v_J defined by $v_J = \Lambda_J\left(\mathcal{R}(\Lambda) \oplus \mathcal{R}(\Lambda)^{\perp}\right)$ satisfy the following properties:

1. $v_J \subset v_{J'} \subset \mathfrak{h}, \quad J < J',$
2. $\overline{\bigcup_{J=-\infty}^{\infty} v_J}^{\,\|\cdot\|_{\mathfrak{h}}} = \mathfrak{h}\,.$

The assertions follow immediately by Definition 3.4 and Theorem 3.5.

4 Reconstruction of Ionospheric Currents from Satellite Data

In the following section we discuss the essential application of this article, the reconstruction of source terms (ionospheric currents) corresponding to given resulting field measurements (magnetic field data measured by satellites). The system of partial differential equations which describes the connection of the source field, g, and the resulting field, f, are the pre-Maxwell equations given by

$$\nabla \wedge f = g \qquad \nabla \cdot f = 0\,,$$

in a certain domain $D \subset \mathbb{R}^3$. For a deduction of this system from the full system of Maxwell's equations the reader is referred to [1]. We assume the domain D to be a spherical shell, i.e. $D = \Omega_{(a,b)}$ and g ought to be vanishing outside $\Omega_{(a,b)}$. The system of partial differential equations is an elliptic problem which is solvable if the inhomogeneity g is known in $\Omega_{(a,b)}$ and boundary values for f are known on Ω_a and Ω_b. For modelling ionospheric current systems and the corresponding magnetic field from given satellite data this assumption, however, is unrealistic because neither the source system g is given anywhere nor the boundary values for f are given on both boundaries.
We are in the situation that magnetic field data are provided on a sphere $\Omega_c \subset \Omega_{(a,b)}$ with $c \in (a, b)$, i.e. lying completely in the ionosphere.

4.1 The Biot-Savart Operator

In the following paragraph we introduce an approach of how the pre-Maxwell problem in spherical geometries can be modelled and modified to be uniquely solvable. We will present the general Biot-Savart operator which is based on Biot-Savart's law of electrodynamics (see e.g. [13]). In order to apply the operator when satellite measurements are concerned we will restrict it to spherical geometries. But at first we give the general definition.

Definition 4.1
Let $g : \mathbb{R}^3 \to \mathbb{R}^3$ be a divergence free, differentiable vector field. Then the *Biot-Savart operator in* $\mathbb{R}^3$, $T : c^{(1)}(\mathbb{R}^3) \to c^{(2)}(\mathbb{R}^3)$, is defined by

$$f(x) = (Tg)(x) = \frac{1}{4\pi} \int_{\mathbb{R}^3} g(y) \wedge \nabla_y \frac{1}{|x-y|}\, dy, \quad x \in \mathbb{R}^3. \tag{12}$$

A simple calculation shows that $Tg(x)$ can be written as follows.

$$Tg(x) = \frac{\mu_0}{4\pi} \int_{\mathbb{R}^3} g(y) \wedge \frac{x-y}{|x-y|^3}\, dy, \quad x \in \mathbb{R}^3. \tag{13}$$

Equation (13) is equivalent to

$$f(x) = \nabla \wedge a(x), \quad x \in \mathbb{R}^3, \tag{14}$$

where

$$a(x) = \frac{1}{4\pi} \int_{\mathbb{R}^3} \frac{g(y)}{|x-y|}\, dy, \quad x \in \mathbb{R}^3. \tag{15}$$

The vector field a is called *vector potential* of g in $\mathbb{R}^3$. Applying the curl to Eq. (14) yields $\nabla \wedge f = g + \nabla(\nabla \cdot a)$. But the last term vanishes in $\mathbb{R}^3$ because of $\nabla \cdot a = 0$ which follows directly from (15) by partial integration and by g to be of zero divergence. Thus, we get that g is the source field of f, provided that f is given by (12).

As we have explained already, this operator is not suitable to cope with the present data situation. We neither know the resulting field nor the source distribution in the whole ionosphere, thus we are not able to solve the direct or the inverse source problem. To overcome this problem let us redefine the Biot-Savart operator in a slightly different manner.

Definition 4.2
Let $R_1, R_2 > 0, R_1 \neq R_2$, be given and let $g : \Omega_{R_1} \to \mathbb{R}^3$ be a vector field of class $l^2(\Omega_{R_1})$. Then the *spherical Biot Savart operator* from Ω_{R_1} to Ω_{R_2}, $T_{R_1,R_2} : l^2(\Omega_{R_1}) \to l^2(\Omega_{R_2})$, is defined by

$$f(x) = (T_{R_1,R_2} g)(x) = \frac{1}{4\pi} \int_{\Omega_{R_1}} g(y) \wedge \frac{x-y}{|x-y|^3} \, d\omega_{R_1}(y), \quad x \in \Omega_{R_2}. \tag{16}$$

Note that in contrast to Definition 4.1 of the Biot-Savart operator T in $\mathbb{R}^3$ we do not require g to be divergence free or surface divergence free here. For the spherical Biot-Savart operator we can immediately state the following lemma.

Lemma 4.3
For the spherical Biot-Savart operator as defined in Definition 4.2 the following properties are valid.

1. *The adjoint operator $T^*_{R_1,R_2} : l^2(\Omega_{R_2}) \to l^2(\Omega_{R_1})$ of T_{R_1,R_2} with respect to the l^2-inner product is given by*
$$T^*_{R_1,R_2} = T_{R_2,R_1}.$$
2. *For $R_1 \neq R_2$ the operator T_{R_1,R_2} is linear, bounded and compact.*
3. *The operator can, for $g \in l^2(\Omega_{R_1})$, be rewritten as*
$$T_{R_1,R_2} g(x) = \left(\nabla_{x'} \wedge \left(\frac{1}{4\pi} \int_{\Omega_{R_1}} \frac{g(y)}{|x'-y|} \, d\omega_{R_1}(y) \right) \right) \Bigg|_{\Omega_{R_2}}. \tag{17}$$

For a proof of this lemma the reader is referred to [17].

The spherical Biot-Savart operator seems to be adequate for modelling the given data situation. It reflects the fact that we have only data on a single sphere from which we want to get as much information as possible. The spherical Biot-Savart operator solves the spherical 'direct source problem' from Ω_{R_1} to Ω_{R_2}, i.e. the operator calculates the vectorial effects on the sphere Ω_{R_2} of a given spherical source distribution on Ω_{R_1}. Its inverse operator $T^{-1}_{R_1,R_2}$, disregarding any existence, uniqueness or continuity statements, solves the spherical 'inverse source problem', i.e. it calculates the vectorial source system on Ω_{R_1} corresponding to a given resulting field on Ω_{R_2}.

By virtue of the compactness of T_{R_1,R_2} we know that the operator has a countable singular system. In order to constitute a multiresolution analysis for the regularization of the inverse problem in the sense of Section 3 we have to calculate the singular system denoted by $\{\sigma_{n'}, h_{n'}, k_{n'}\}$ of the operator $T_{R_1,R_2} : \mathfrak{h} = l^2(\Omega_{R_1}) \to \mathfrak{k} = l^2(\Omega_{R_2})$ explicitly.

Theorem 4.4
Let the system of vector spherical harmonics be given as in Lemma 2.2.
Then we have for $R_2 < R_1$

$$T_{R_1,R_2} u_{n,k}^{(1),R_1} = -\sqrt{\frac{n}{2n+1}} \left(\frac{R_2}{R_1}\right)^{n+1} u_{n,k}^{(3),R_2}, \tag{18}$$

$$T_{R_1,R_2} u_{n,k}^{(2),R_1} = 0, \tag{19}$$

$$T_{R_1,R_2} u_{n,k}^{(3),R_1} = -\sqrt{\frac{n+1}{2n+1}} \left(\frac{R_2}{R_1}\right)^{n} u_{n,k}^{(2),R_2}, \tag{20}$$

while for $R_2 > R_1$

$$T_{R_1,R_2} u_{n,k}^{(1),R_1} = 0, \tag{21}$$

$$T_{R_1,R_2} u_{n,k}^{(2),R_1} = -\sqrt{\frac{n+1}{2n+1}} \left(\frac{R_1}{R_2}\right)^{n} u_{n,k}^{(3),R_2}, \tag{22}$$

$$T_{R_1,R_2} u_{n,k}^{(3),R_1} = -\sqrt{\frac{n}{2n+1}} \left(\frac{R_1}{R_2}\right)^{n+1} u_{n,k}^{(1),R_2}, \tag{23}$$

For a proof of this theorem the reader is referred to [17]. The proof is mainly based on the decomposition of the system $\{u_{n,k}^{(i)}\}$ in terms of the system $\{y_{n,k}^{(i)}\}$ and the representation of the Biot-Savart operator as the curl of a vectorial double-layer potential given in (17). To be more specific, the expansion of the fundamental solution of the Laplace operator, $1/|x-y|$, in terms of Legendre polynomials and a vectorial Funk-Hecke formula are used, which both can be found in [8].

Physically interpreted Corollary 4.4 connects the components of a spherical current system to the corresponding magnetic field at a different height. In other words the corollary states that current systems of class $l_{\mathcal{U}}^{2,(2)}(\Omega_{R_1})$ induce no magnetic field inside the sphere, where they are present and current systems of class $l_{\mathcal{U}}^{2,(1)}(\Omega_{R_1})$ produce no magnetic field outside the sphere Ω_{R_1}. This is a generalized mathematical form of a result presented in [11] which states that spherical poloidal currents produce no magnetic field inside the sphere where they are present.

Observing that $T_{R_1,R_2}^* = T_{R_2,R_1}$ and combining the results of the previous theorem yields

Corollary 4.5
Let the system of vector spherical harmonics be given as in Lemma 2.2.

Then we have for $R_2 < R_1$

$$T^*_{R_1,R_2} T_{R_1,R_2} u^{(1),R_1}_{n,k} = \frac{n}{2n+1} \left(\frac{R_2}{R_1}\right)^{2n+2} u^{(1),R_1}_{n,k}, \tag{24}$$

$$T^*_{R_1,R_2} T_{R_1,R_2} u^{(2),R_1}_{n,k} = 0, \tag{25}$$

$$T^*_{R_1,R_2} T_{R_1,R_2} u^{(3),R_1}_{n,k} = \frac{n+1}{2n+1} \left(\frac{R_2}{R_1}\right)^{2n} u^{(3),R_1}_{n,k}, \tag{26}$$

and for $R_2 > R_1$

$$T^*_{R_1,R_2} T_{R_1,R_2} u^{(1),R_1}_{n,k} = 0, \tag{27}$$

$$T^*_{R_1,R_2} T_{R_1,R_2} u^{(2),R_1}_{n,k} = \frac{n+1}{2n+1} \left(\frac{R_1}{R_2}\right)^{2n} u^{(2),R_1}_{n,k}, \tag{28}$$

$$T^*_{R_1,R_2} T_{R_1,R_2} u^{(3),R_1}_{n,k} = \frac{n}{2n+1} \left(\frac{R_1}{R_2}\right)^{2n+2} u^{(3),R_1}_{n,k}, \tag{29}$$

Since we deal with the situation that resulting field measurements are given on a sphere which is above the source field, we are mainly interested in the last three equations of Corollary 4.5 and in Eq. (21 - 23) of Theorem 4.4.

Eq. (18 - 20) and Eq. (21 - 23) now establish the starting point to apply the multiscale regularization techniques for vectorial inverse problems which has been developed in Section 3. The singular system of the Biot-Savart operator $T_{R_1,R_2} : \mathfrak{h} \to \mathfrak{k}$, for $R_2 < R_1$, is given in Table 1 and, for $R_1 < R_2$, in Table 2.

$\mathfrak{h}$	$\mathfrak{k}$	$\{h_n\}$	$\{k_n\}$	σ_n
$l^{2,(1)}_{\mathcal{U}}(\Omega_{R_1})$	$l^{2,(3)}_{\mathcal{U}}(\Omega_{R_2})$	$u^{(1),R_1}_{n,k}$	$-u^{(3),R_2}_{n,k}$	$\sqrt{\frac{n}{2n+1}} \left(\frac{R_2}{R_1}\right)^{n+1}$
$l^{2,(3)}_{\mathcal{U}}(\Omega_{R_1})$	$l^{2,(2)}_{\mathcal{U}}(\Omega_{R_2})$	$u^{(3),R_1}_{n,k}$	$-u^{(2),R_2}_{n,k}$	$\sqrt{\frac{n+1}{2n+1}} \left(\frac{R_2}{R_1}\right)^{n}$

Table 1: Singular system of the spherical Biot-Savart operator $T_{R_1,R_2} : \mathfrak{h} \to \mathfrak{k}$ for the case $R_2 < R_1$.

$\mathfrak{h}$	$\mathfrak{k}$	$\{h_n\}$	$\{k_n\}$	σ_n
$l^{2,(2)}_{\mathcal{U}}(\Omega_{R_1})$	$l^{2,(3)}_{\mathcal{U}}(\Omega_{R_2})$	$u^{(2),R_1}_{n,k}$	$-u^{(3),R_2}_{n,k}$	$\sqrt{\frac{n+1}{2n+1}} \left(\frac{R_1}{R_2}\right)^{n}$
$l^{2,(3)}_{\mathcal{U}}(\Omega_{R_1})$	$l^{2,(1)}_{\mathcal{U}}(\Omega_{R_2})$	$u^{(3),R_1}_{n,k}$	$-u^{(1),R_2}_{n,k}$	$\sqrt{\frac{n}{2n+1}} \left(\frac{R_1}{R_2}\right)^{n+1}$

Table 2: Singular system of the spherical Biot-Savart operator $T_{R_1,R_2} : \mathfrak{h} \to \mathfrak{k}$ for the case $R_2 > R_1$.

It is obvious that the singular values of the Biot-Savart operator given in Table 1 and Table 2 constitute an exponentially ill posed problem. In order to force convergence we

have to replace the generalized inverse by a filtered version of this expansion. This has been done in Section 3 in a general multiscale framework for regularization of vectorial inverse problems (see e.g. [6] or [15]).

5 An Application to CHAMP Magnetic Field Data

The morphology of the geomagnetic variations produced by ionospheric currents can only weakly be represented in a coordinate system which is Earth fixed. This is because the magnetic field induced by currents is not linked to geographical longitude and latitude as, for example, is the lithospheric field. It is rather fixed to the position of the Sun and the distance of the observer (in this case the satellite) to the geomagnetic equator. Thus, in order to describe these phenomena we have to change the reference system from an Earth fixed frame to a Sun fixed frame. A coordinate system which is commonly used in geophysics in this context is the Magnetic Local Time (MLT) and Quasi Dipole Latitude (QDlat). The magnetic local time thereby denotes the relative position of the observer with respect to the magnetic field and the Sun and the quasi dipole latitude represents the relative position of the observer with respect to the geomagnetic equator. For more information concerning the description of geomagnetic coordinate system the reader is referred to [20] and the reference therein.

5.1 An Application to CHAMP Magnetic Field Data

To show that our method is able to handle data in this coordinate system we take just three days of CHAMP (a German geosientific research satellite operated by the GFZ Potsdam) magnetic field data (10., 20. and 21. September 2001) which where available at the internet page `http://www.dsri.dk/multimagsatellites /types/equatorial_electrojet.html`. In these days CHAMP was at 12.30 and 00.30 local time. The data are averaged to an equiangular integration grid (in the coordinate system (MLT, QDlat)) using an algorithm presented in [17]. The reference system (MLT, QDlat), with values $QDlat \in [-90, 90]$ and $MLT \in [0, 24]$ is thereby just seen as another coordinate system parameterizing the unit sphere where the magnetic local time is seen as a linear transformation of the longitude with $MLT = 12$ representing the zero meridian.

We apply the method presented in the previous section to the CHAMP data set in order to reconstruct the toroidal part contained in $l^{2,(3)}_{\mathcal{U}}(\Omega_{R_1})$ of the equivalent ionospheric current system from the poloidal part of the magnetic field measurements. Since we are in the case of $R_2 > R_1$, Eq. (21) of Corollary 4.4 plays the essential role in our regularization step. The functional-analytic framework is given as follows. We have to regularize the inversion of $T_{R_1,R_2} : \mathfrak{h} \to \mathfrak{k}$, where T_{R_1,R_2} is the spherical Biot-Savart operator given in Definition 4.2 and

$$\begin{aligned} \mathfrak{h} &= l^{2,(3)}_{\mathcal{U}}(\Omega_{R_1}), \quad \{h_{n'}\} = \{-u^{(3),R_1}_{n,k}\}_{\substack{n=1,\dots;\\ k=1,\dots,2n+1}}, \\ \mathfrak{k} &= l^{2,(1)}_{\mathcal{U}}(\Omega_{R_2}), \quad \{k_{n'}\} = \{u^{(1),R_2}_{n,k}\}_{\substack{n=1,\dots;\\ k=1,\dots,2n+1}}, \\ \sigma_{n'} &= \sqrt{\frac{n}{2n+1}} \left(\frac{R_1}{R_2}\right)^{n+1}, \qquad n' \in \mathbb{N}\,. \end{aligned}$$

The result of our reconstruction with a regularization vector cubic polynomial scaling function at scale $J = 3$ can be seen in Figure 5.1. The maximal strength of the detected equivalent ionospheric current system is approximately $10\,mA/m$. According to [3] the amplitude of the solar quiet mid latitude ionospheric current systems is $10 - 36\,mA/m$. This shows that the detected current system is in the lower band width of the real ionospheric current systems. Since the scale of reconstruction is very low it can be assumed that the real strength of the current system is higher than the reconstructed amplitude.

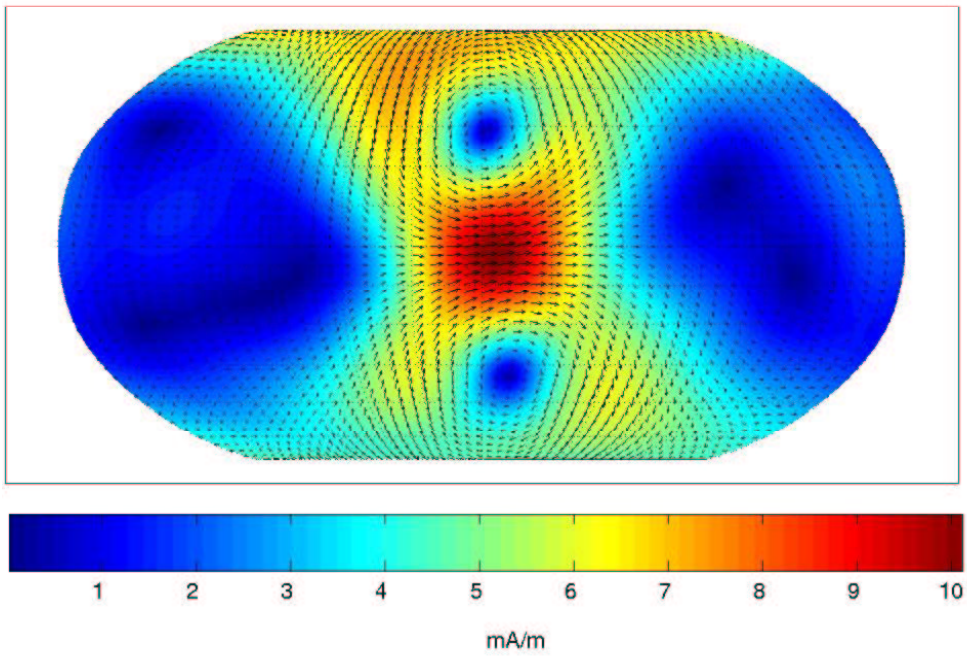

Figure 1: Equivalent horizontal current distribution in the Sun fixed coordinate system (QDlat, MLT) at a height of $110\,km$ calculated using a regularization vector cubic polynomial scaling function expansion at scale $J = 3$.

With respect to the given amount of data (3 days of CHAMP magnetic field measurements) the reconstructed current system shown in Figure 5.1 is a remarkable result. It demonstrates that the used trial functions, i.e. regularization vector scaling functions and wavelets, are an adequate choice for handling the problem. As already mentioned in [14] the main disadvantage of spherical harmonics is that the reconstructed current system on the day-side of the Earth will appear on the night-side as well because of symmetry arguments. This problem does not appear if scaling functions and wavelets are used. These kernel functions do not fulfill an exact frequency localization property which is not needed for the reconstruction of the current system anyway, but they provide the possibility of space localizing reconstruction and this property is much more important for the reconstruction of a ionospheric current distribution from given magnetic field measurements.

In order to demonstrate the regional applicability of the presented multiscale techniques for reconstructing ionospheric current systems from CHAMP magnetic field data we calculate the toroidal part of the equivalent ionospheric current system at a height of 110 km from CHAMP magnetic field measurements. The local reconstruction is performed in a

region given by $QDlat \in [-30, 30]$ and $MLT \in [08.00, 16.00]$, i.e. in an area, where strong ionospheric current systems like the equatorial electrojet are present. For this reconstruction we took data of several months between September 2001 and June 2002 in order to get an appropriate coverage of measurements in the region of interest. For further information concerning data selection and preprocessing steps see [17].

The reconstruction of the equivalent ionospheric current system with a regularization vector cubic polynomial scaling function at scale $J = 5$ can be seen in Figure 2. The maximal reconstructed strength of the current system is approximately 25 mA/m which is a more realistic value than the amplitude of the reconstruction in Figure 5.1.

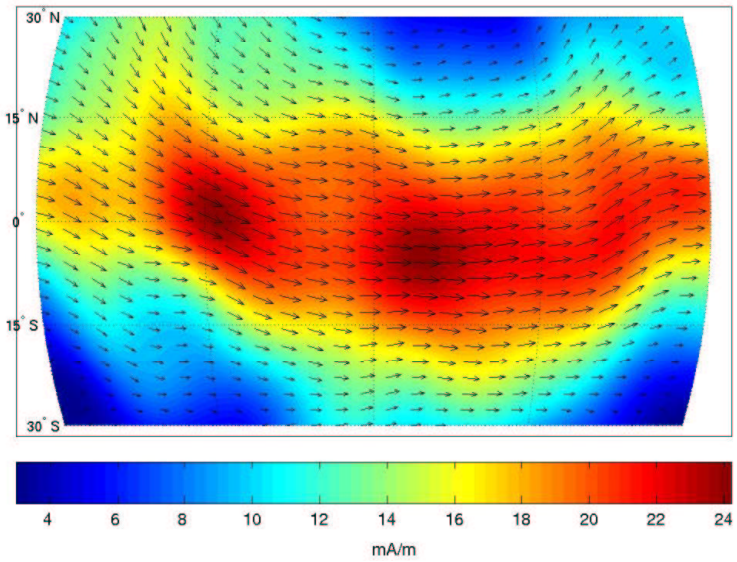

Figure 2: Local reconstruction ($QDlat \in [-30, 30]$, $MLT \in [08.00, 16.00]$) of the equivalent ionospheric current distribution at a height of 110 km calculated using a regularization vector cubic polynomial scaling function expansion at scale $J = 5$.

5.2 An Application to SWARM Magnetic Field Data

In the following section we give an example how the multiscale method of reconstructing current systems from magnetic field data can be used in connection with the proposed satellite mission SWARM.
SWARM is a satellite mission proposed by a consortium of 27 institutes and universities under the leadership of the Danish Space Research Institute (DSRI Kopenhagen). It is designed to study the dynamics of the Earth's magnetic field and its interactions with the system Earth. The concept consists of a constellation of four satellites of the CHAMP type in two different polar orbits between 400 km and 550 km altitude. To simulate the SWARM mission and the emphasize its advantages a simulator (based on the comprehensive model of the near-Earth magnetic field described in [21]) has been implemented at the GFZ Potsdam and the data has been made available at the DSRI Kopenhagen.
To test our method with a big amount of satellite data we took 60 days of data between January 2000 and April 2000 of one of the low flying SWARM satellite's. The period of 4 months is necessary to get data within all magnetic local times. As before the data

is transformed to the (MLT, QDlat) coordinate system and averaged to an equiangular integration grid (in the coordinate system (MLT, QDlat)).

The ionospheric current system which has been used to simulate SWARM magnetic field data is a purely toroidal, horizontal current system at a height of 110 km (see [21]). Thus, in order to apply our method to reconstruct the current system corresponding to the simulated magnetic field data we are in the same functional-analytic situation as in the previous subsection.

A reconstructed equivalent ionospheric current system at a height of 110 km obtained with a regularization cubic polynomial vector scaling function at scale $J = 5$ can be found in Figure 3. The main contours of the ionospheric current system are reconstructed. In order to reconstruct finer details of the current system a higher resolution of the simulated satellite tracks (at the moment 1 sample/min $\simeq$ 440 km sample distance) would be necessary. The corresponding current function of the current system presented in Figure 3 which can easily be reconstructed in the multiscale framework presented in this article (see [17] for more details) can be found in Figure 4.

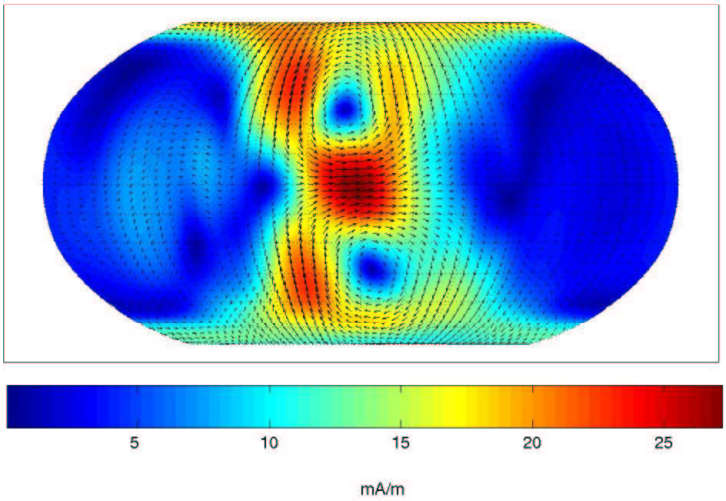

Figure 3: Equivalent horizontal current distribution in the Sun fixed coordinate system (QDlat, MLT) at a height of 110 km calculated using a regularization vector cubic polynomial scaling function expansion at scale $J = 5$.

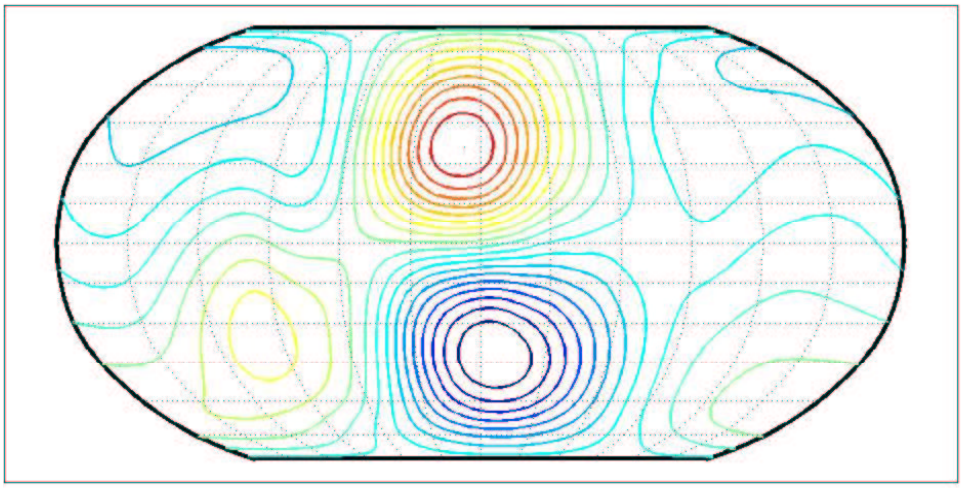

Figure 4: Equipotential lines of the current function of the equivalent horizontal current distribution in the Sun fixed coordinate system (QDlat, MLT) calculated using a regularization scalar cubic polynomial scaling function at scale $J = 5$. Red indicates the maximum strength of the current function while blue indicates the minimum.

Acknowledgements

I want to thank the Graduiertenkolleg "Mathematik und Praxis" for financial support. Many helpful comments and discussions with W. Freeden, T. Maier (Geomathematics Group, TU Kaiserslautern) and H. Lühr (GFZ Potsdam) as well as comments from M.Z. Nashed at the AMS Conference 2003, Baltimore, and I.H. Sloan at ICIAM03, Sydney, are gratefully acknowledged.

References

[1] G.E. Backus, R. Parker, and C. Constable. *Foundations of Geomagnetism.* Cambridge University Press, Cambridge, 1996.

[2] M. Bayer, S. Beth, and W. Freeden. Geophysical field modelling by multiresolution analysis. *Acta Geod. Geoph. Hung.*, 33(2-4):289–319, 1998.

[3] W.H. Cambell. *Quit Daily Geomagnetic Fields.* Birkhäuser Verlag, 1989.

[4] P.J. Davis. *Interpolation and Approximation.* Dover Publications Inc., New York, 1975.

[5] A.R. Edmonds. *Angular Momentum in Quantum Mechanics.* Princeton University Press, 1957.

[6] H.W. Engl, M. Hanke, and A. Neubauer. *Regularization of Inverse Problems.* Kluwer, Dordrecht, Boston, London, 1996.

[7] W. Freeden. *Multiscale Modelling of Spaceborne Geodata.* B.G. Teubner, Stuttgart, Leipzig, 1999.

[8] W. Freeden, T. Gervens, and M. Schreiner. *Constructive Approximation on the Sphere (With Applications to Geomathematics)*. Oxford Science Publications, Clarendon, 1998.

[9] W. Freeden and T. Maier. Spectral and multiscale signal-to-noise thresholding of spherical vector fields. *Computational Geosciences*, 7(3):215–250, 2003.

[10] W. Freeden and F. Schneider. Regularization wavelets and multiresolution. *Inverse Problems*, 14:225–243, 1998.

[11] N. Fukushima. Generalized theorem for no ground magnetic effect of vertical currents connected with pedersen currents in the uniform-conductivity ionosphere. *Rep. Ionos. Space Res. Jpn.*, 30:35–40, 1976.

[12] C. F. Gauss. Allgemeine Theorie des Erdmagnetismus. Resultate aus den Beobachtungen des magnetischen Vereins im Jahre 1838 (English translation: General theory of terrestrial magnetism). In R. Taylor, editor, *Scientific Memoirs Selected from the Transactions of Foreign Academies of Science and Learned Societies and from Foreign Journals*, volume 2, pages 184–251, 1841.

[13] J.D. Jackson. *Classical Electrodynamics*. John Wileys and Sons, 1975.

[14] W. Kertz. *Einführung in die Geophysik 2*. B.I. Hochschultaschenbücher, Mannheim, Wien, Zürich, 1969.

[15] A.K. Louis. *Inverse und schlecht gestellte Probleme*. Teubner, Stuttgart, 1989.

[16] T. Maier. *Multiscale Geomagnetic Field Modelling from Satellite Data: Theoretical Aspects and Numerical Application*. PhD thesis, Geomathematics Group, Department of Mathematics, University of Kaiserslautern, 2003.

[17] C. Mayer. *Wavelet Modelling of Ionospheric Currents and Induced Magnetic Fields From Satellite Data*. PhD thesis, Geomathematics Group, Department of Mathematics, University of Kaiserslautern., 2003.

[18] V. Michel. *A Multiscale Approximation for Operator Equations in Separable Hilbert Spaces – Case Study: Reconstruction and Description of the Earth's Interior*. Habilitation, Geomathematics Group, Department of Mathematics, University of Kaiserslautern, 2002.

[19] H. Nutz. *A Unified Setup of Gravitational Field Observables*. PhD thesis, Geomathematics Group, Department of Mathematics, University of Kaiserslautern. Shaker, Aachen, 2002.

[20] A.D. Richmond. Ionspheric electrodynamics using magnetic apex coordinates. *J. Geomag. Geoelec.*, 47:191–212, 1995.

[21] T.J. Sabaka, N. Olsen, and R.A. Langel. A Comprehensive Model of the Near-Earth Magnetic Field: Phase 3. *NASA/TM-2000-209894*, 2000.

Folgende Berichte sind erschienen:

2003

Nr. 1 S. Pereverzev, E. Schock.
On the adaptive selection of the parameter in regularization of ill-posed problems

Nr. 2 W. Freeden, M. Schreiner.
Multiresolution Analysis by Spherical Up Functions

Nr. 3 F. Bauer, W. Freeden, M. Schreiner.
A Tree Algorithm for Isotropic Finite Elements on the Sphere

Nr. 4 W. Freeden, V. Michel (eds.)
Multiscale Modeling of CHAMP-Data

Nr. 5 C. Mayer
Wavelet Modelling of the Spherical Inverse Source Problem with Application to Geomagnetism

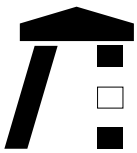

TECHNISCHE UNIVERSITÄT
KAISERSLAUTERN

Informationen:

Prof. Dr. W. Freeden
Prof. Dr. E. Schock
Fachbereich Mathematik
Technische Universität Kaiserslautern
Postfach 3049
D-67653 Kaiserslautern
E-Mail: freeden@mathematik.uni-kl.de
schock@mathematik.uni-kl.de